Wavelength Multistability in Lasers: The Effect of Spatial Hole Burning

Antonio Pérez-Serrano[(1)], Julien Javaloyes[(2)]
and Salvador Balle[(3)]

(1) IFISC (UIB-CSIC), Palma de Mallorca, Spain
(2) Departament de Física, UIB, Palma de Mallorca, Spain
(3) IMEDEA (UIB-CSIC), Esporles, Spain

IFISC

CSIC UIB

Outline

I. Motivation

II. The model

III. Longitudinal modal multistability in lasers:
Comparison between Ring and Fabry-Pérot configurations

IV. Conclusions

I. Motivation

- Ring Lasers can exhibit a rich variety of dynamical regimes:

Bidirectional CW
Alternate Oscillations
Modelocking
Bistability
Chaos
...

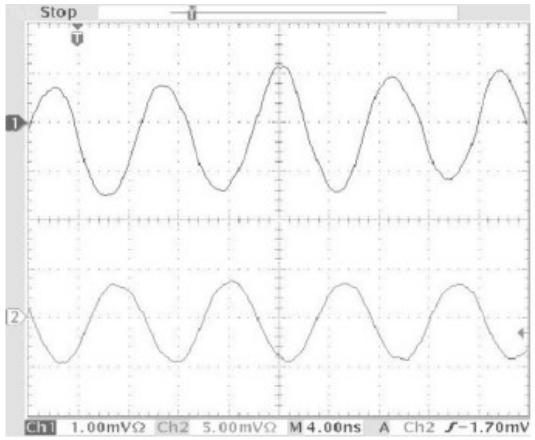

Sorel et al.
IEEE JQE **39**, 1187 (2003)

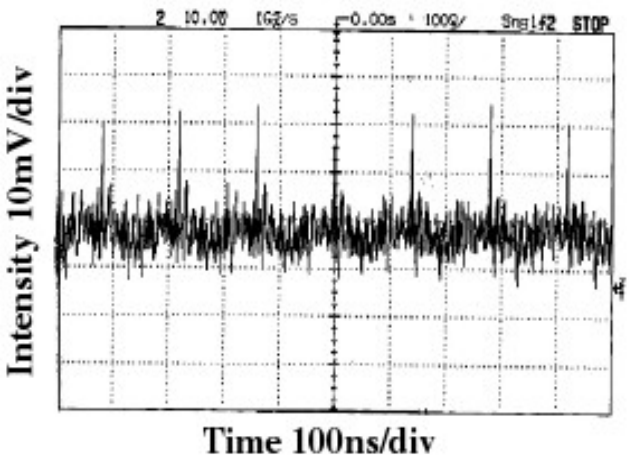

Zhang et al.
J. Opt. A. **7**, 175 (2005)

I. Motivation

- Ring Lasers can exhibit a rich variety of dynamical regimes:

Bidirectional CW
Alternate Oscillations
Modelocking
Bistability
Chaos
...

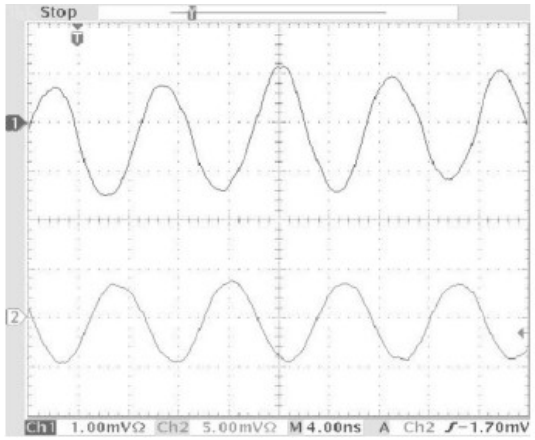

Sorel et al.
IEEE JQE **39**, 1187 (2003)

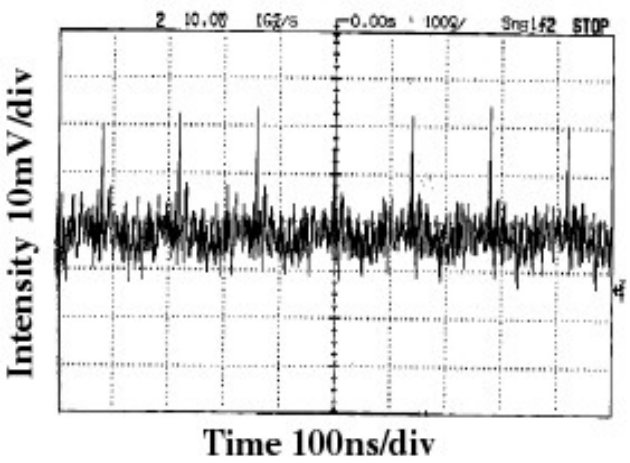

Zhang et al.
J. Opt. A. **7**, 175 (2005)

Bistability in directional emission ⟶ **All-optical binary logics**

Hill et al. Nature **432**, 206 (2004)

I. Motivation

- Experimental results show that in SRLs emission wavelength can be selected by optical injection, and the system remains stable at the chosen value.

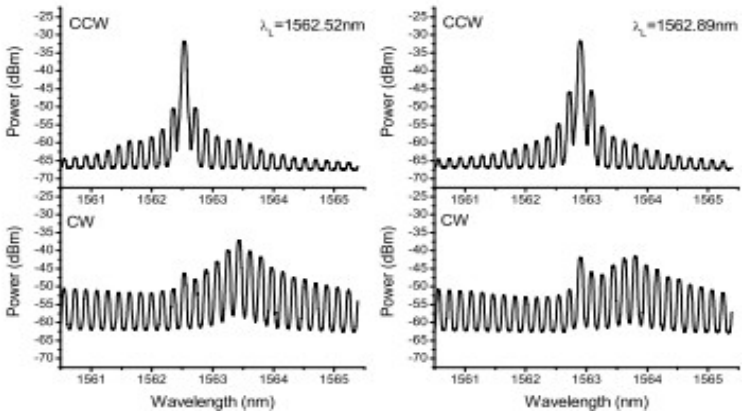

Born et al. IEEE JQE **41**, 261 (2005).

All-optical higher order logics

I. Motivation

- Experimental results show that in SRLs emission wavelength can be selected by optical injection, and the system remains stable at the chosen value.

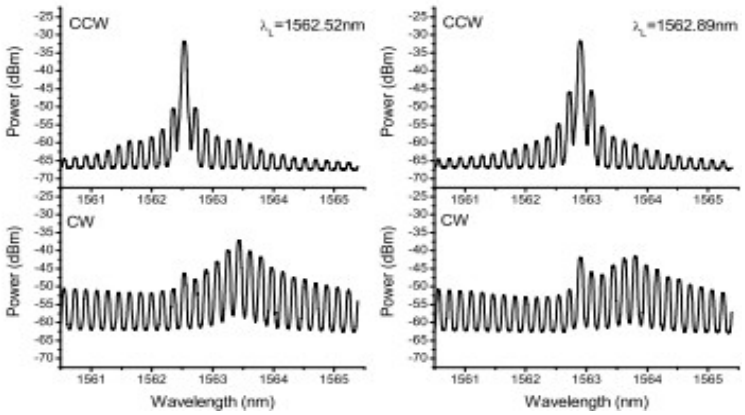

Born et al. IEEE JQE **41**, 261 (2005).

All-optical higher order logics

- Existing Models: Rate Equations-Like (ODEs)
  Spatial dependence simplified

Modal couplings??

I. Motivation

- Experimental results show that in SRLs emission wavelength can be selected by optical injection, and the system remains stable at the chosen value.

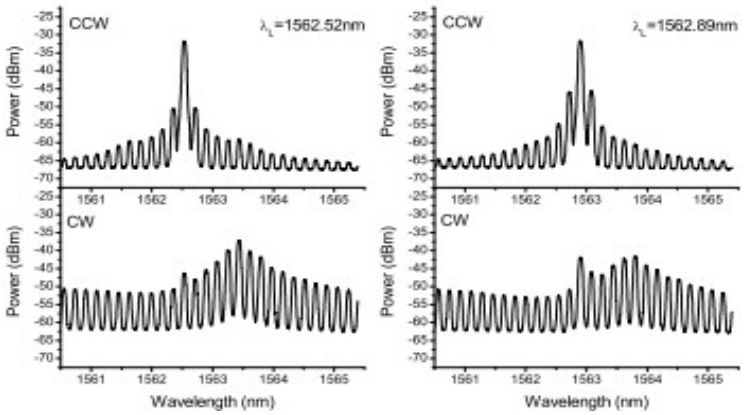

Born et al. IEEE JQE **41**, 261 (2005).

All-optical higher order logics

- Existing Models: Rate Equations-Like (ODEs)
  Spatial dependence simplified

Modal couplings??

- Comprehensive theory ⟶ Taking into account spatial effects / Modal couplings

- Generality of the TWM : Description of different types of lasers.
  (PDEs) Multimode behavior arises naturally in a TWM description.

II. The model

Dimensionless TW Equations
for the SVA in a Semi-classical approach:

$$\pm\frac{\partial A_\pm}{\partial s}+\frac{\partial A_\pm}{\partial \tau}=B_\pm-\alpha A_\pm$$ Electric Fields

II. The model

Dimensionless TW Equations
for the SVA in a Semi-classical approach:

$$\pm\frac{\partial A_\pm}{\partial s}+\frac{\partial A_\pm}{\partial \tau}=B_\pm-\alpha A_\pm$$ Electric Fields

$$\frac{1}{\gamma}\frac{\partial B_\pm}{\partial \tau}=-(1+i\tilde{\delta})B_\pm+g(D_0A_\pm+D_{\pm 2}A_\mp)+\sqrt{\beta D_0}\xi_\pm(s,\tau)$$ Polarization

$$\frac{\partial D_0}{\partial \tau}=\epsilon[J-D_0+\Delta\frac{\partial^2 D_0}{\partial s^2}-(A_+B_+^*+A_-B_-^*+A_+^*B_++A_-^*B_-)]$$

$$\frac{\partial D_{\pm 2}}{\partial \tau}=-\eta D_{\pm 2}-\epsilon(A_\pm B_\mp^*+A_\mp^*B_\pm)$$

Carriers

II. The model

Dimensionless TW Equations
for the SVA in a Semi-classical approach:

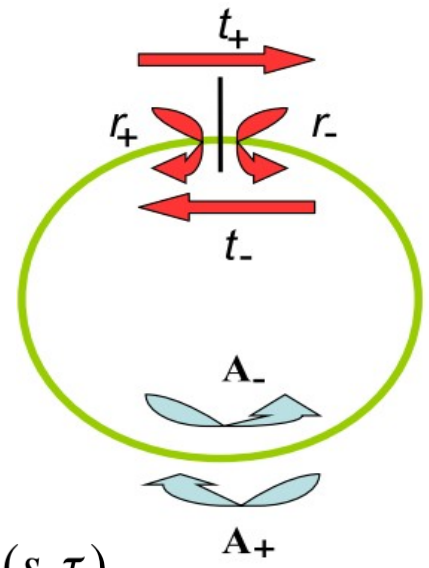

$$\pm\frac{\partial A_\pm}{\partial s}+\frac{\partial A_\pm}{\partial \tau}=B_\pm-\alpha A_\pm$$ Electric Fields

$$\frac{1}{\gamma}\frac{\partial B_\pm}{\partial \tau}=-(1+i\tilde{\delta})B_\pm+g(D_0A_\pm+D_{\pm 2}A_\mp)+\sqrt{\beta D_0}\xi_\pm(s,\tau)$$ Polarization

$$\frac{\partial D_0}{\partial \tau}=\epsilon[J-D_0+\Delta\frac{\partial^2 D_0}{\partial s^2}-(A_+B_+^*+A_-B_-^*+A_+^*B_++A_-^*B_-)]$$

$$\frac{\partial D_{\pm 2}}{\partial \tau}=-\eta D_{\pm 2}-\epsilon(A_\pm B_\mp^*+A_\mp^*B_\pm)$$

} Carriers

Boundary Conditions:

$$A_+(0,\tau)=t_+A_+(1,\tau)+r_-A_-(0,\tau)$$
$$A_-(1,\tau)=t_-A_-(0,\tau)+r_+A_+(1,\tau)$$

FP : $t_\pm = 0$

Ideal Ring: $r_\pm = 0$

II. The model

Solving PDEs numerically:

Fleck, Phys. Rev. B **1**, 84 (1970).

Tests for the numerical algorithm:

Analytical Results (Unidirectional or UFL)

Zeghlache et al. Phys. Rev. A **37**, 470 (1988).

II. The model

Solving PDEs numerically:

Fleck, Phys. Rev. B **1**, 84 (1970).

Tests for the numerical algorithm:

Analytical Results (Unidirectional or UFL)

Zeghlache et al. Phys. Rev. A **37**, 470 (1988).

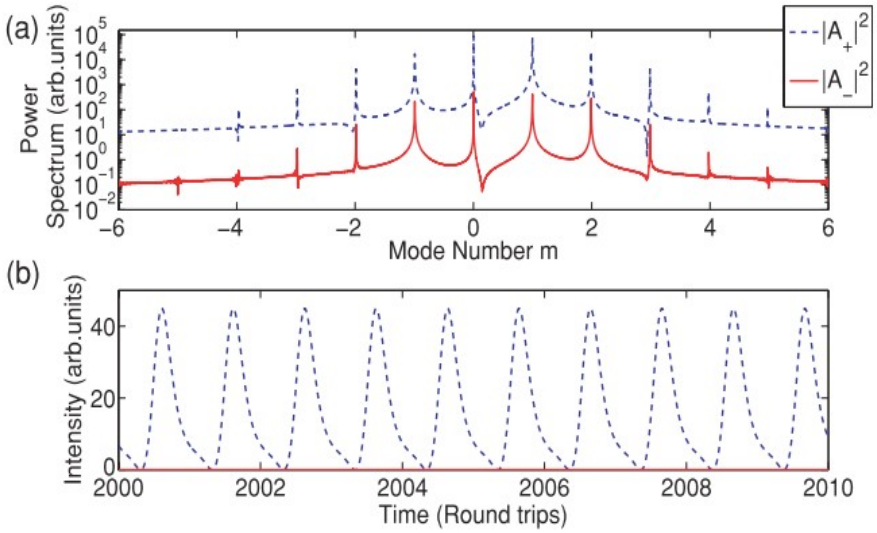

For details: C2.4 Talk 9:30h

II. The model

Solving PDEs numerically:

Fleck, Phys. Rev. B **1**, 84 (1970).

Tests for the numerical algorithm:

Analytical Results (Unidirectional or UFL)

Zeghlache et al. Phys. Rev. A **37**, 470 (1988).

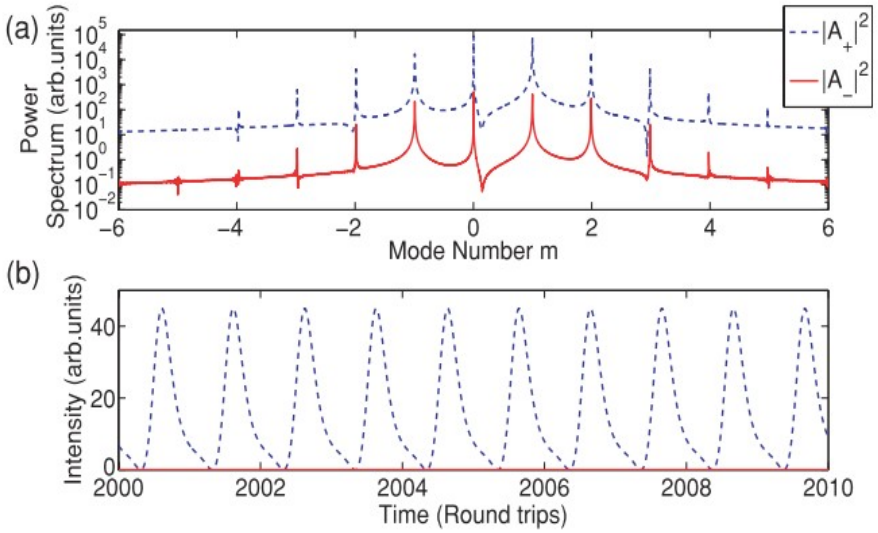

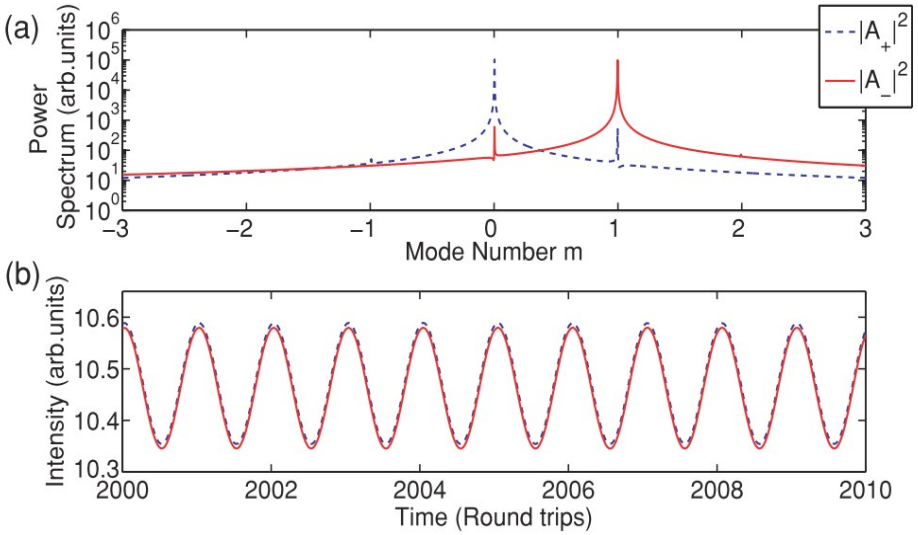

For details: C2.4 Talk 9:30h

III. Longitudinal modal multistability in lasers

Ascertaining multistability → Monochromatic solutions Eigenvalue problem → Analytically difficult in the general case

III. Longitudinal modal multistability in lasers

Ascertaining multistability → Monochromatic solutions Eigenvalue problem → Analytically difficult in the general case

- Monochromatic Solutions via a low dimensional shooting method.
  → Discretized representation of the modal profile.

III. Longitudinal modal multistability in lasers

Ascertaining multistability → Monochromatic solutions Eigenvalue problem → Analytically difficult in the general case

- Monochromatic Solutions via a low dimensional shooting method.
  → Discretized representation of the modal profile.

- Eigenvalue Problem:
  - Hyperbolic PDE: discrete representation of the gradient
    → Large error in the computed eigenvalues.

III. Longitudinal modal multistability in lasers

Ascertaining multistability → Monochromatic solutions Eigenvalue problem → Analytically difficult in the general case

- Monochromatic Solutions via a low dimensional shooting method.
  → Discretized representation of the modal profile.

- Eigenvalue Problem:
  - Hyperbolic PDE: discrete representation of the gradient
    → Large error in the computed eigenvalues.

- Linearized evolution operator → Floquet multipliers

- This approach is quite general: can be used in other dynamical systems with PDEs.

III. Longitudinal modal multistability in lasers

Bidirectional Ring laser

LSA for mode m = 2

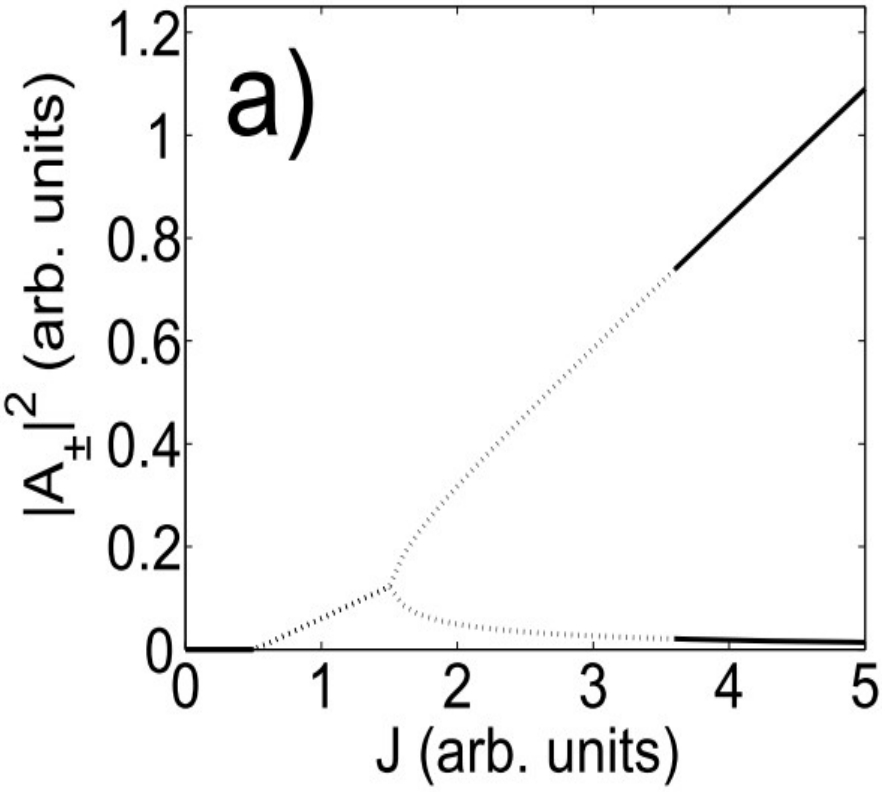

$g = 4$
$t_{\pm} = 0.98$
$r_{\pm} = 0.01$
$\varepsilon = 0.05$
$\eta = 10$
$\gamma = 250$
$\Delta = 0$
$\alpha = 2.03$

Typical parameters for semiconductor lasers

III. Longitudinal modal multistability in lasers

Bidirectional Ring laser

LSA for mode m = 2

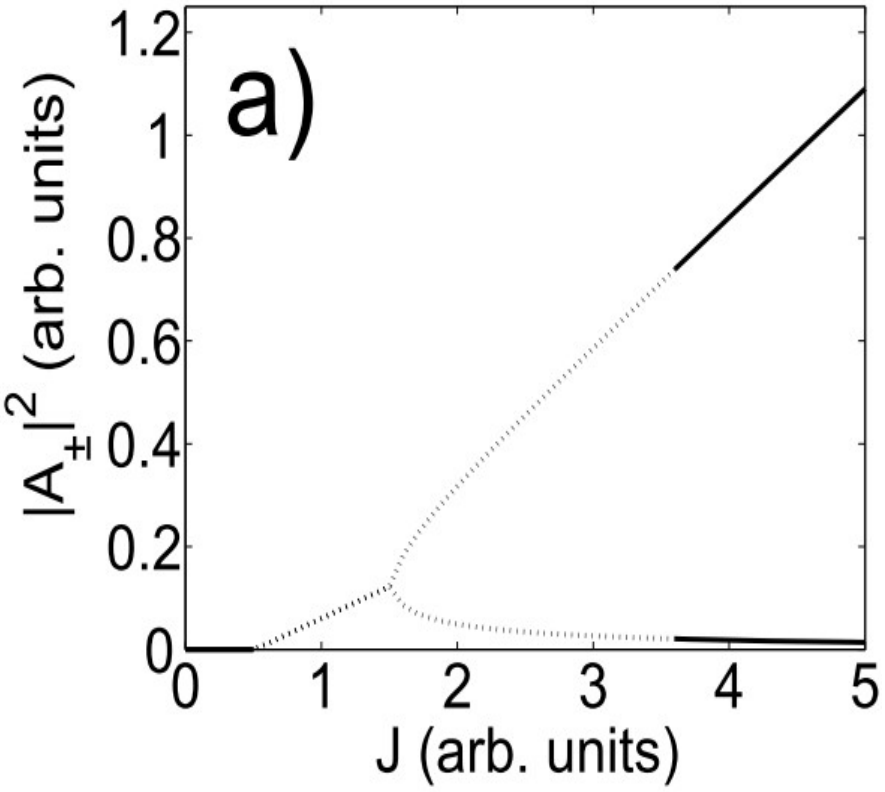

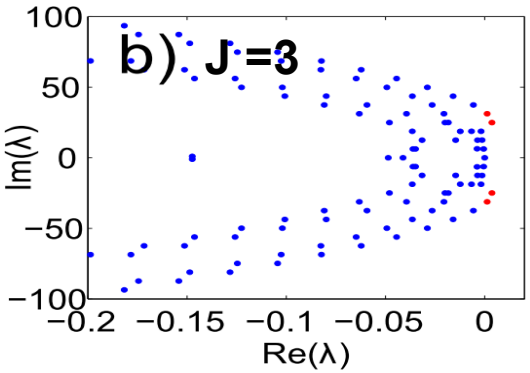

$g = 4$

$t_{\pm} = 0.98$

$r_{\pm} = 0.01$

$\varepsilon = 0.05$

$\eta = 10$

$\gamma = 250$

$\Delta = 0$

$\alpha = 2.03$

Typical parameters for semiconductor lasers

III. Longitudinal modal multistability in lasers

Bidirectional Ring laser

LSA for mode m = 2

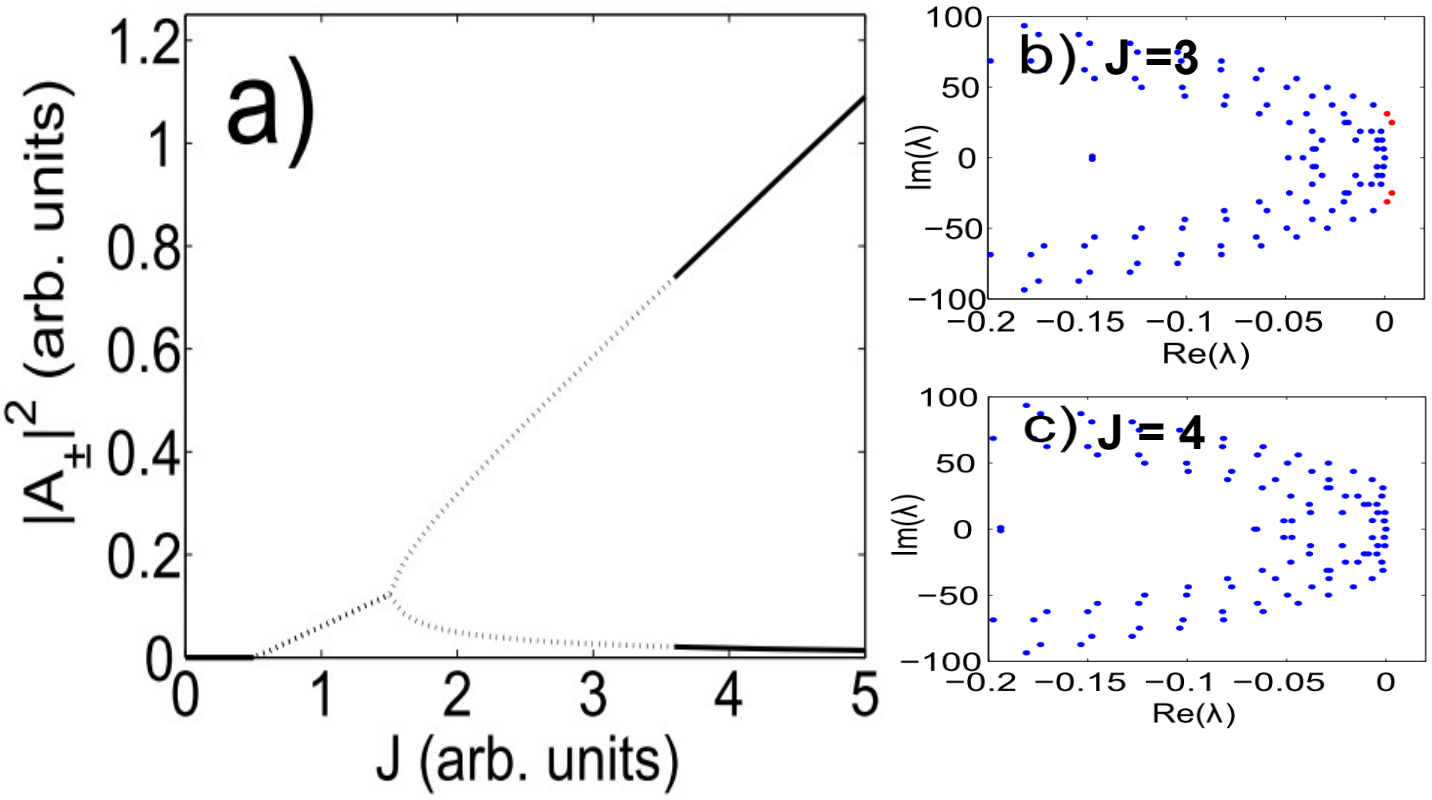

$g = 4$
$t_\pm = 0.98$
$r_\pm = 0.01$
$\varepsilon = 0.05$
$\eta = 10$
$\gamma = 250$
$\Delta = 0$
$\alpha = 2.03$

Typical parameters for semiconductor lasers

III. Longitudinal modal multistability in lasers

Uniform Field Limit (UFL)

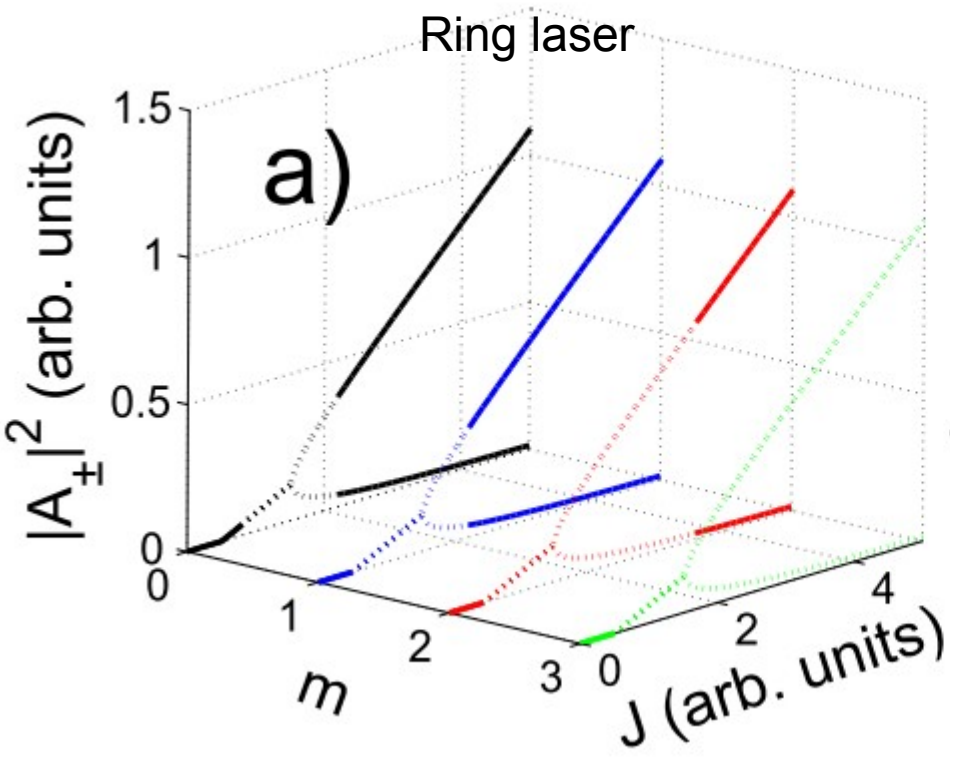

III. Longitudinal modal multistability in lasers

Uniform Field Limit (UFL)

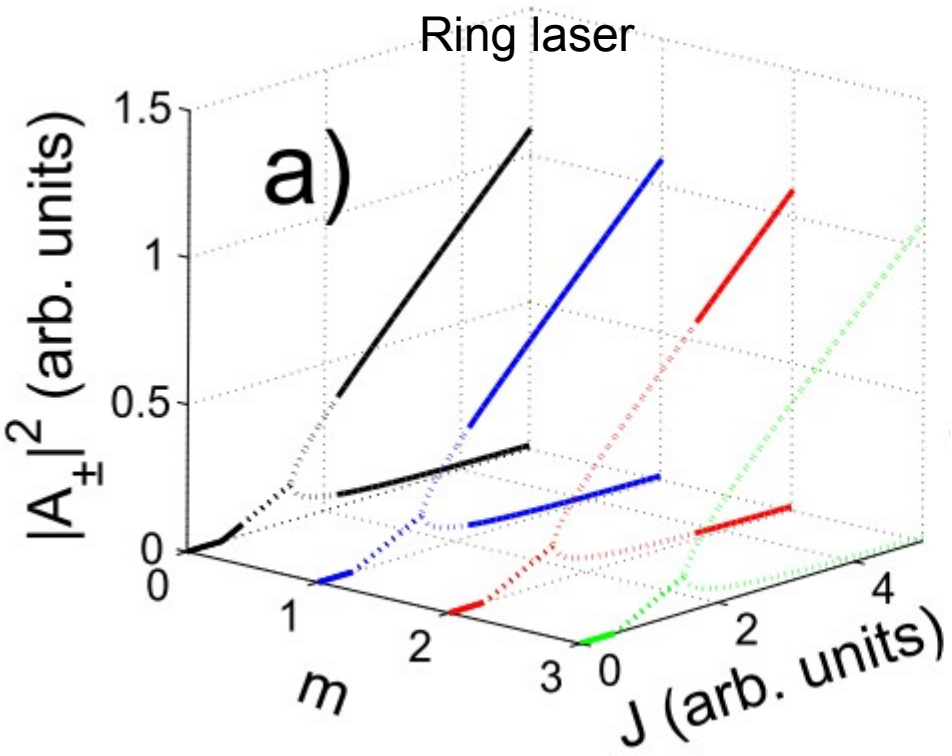

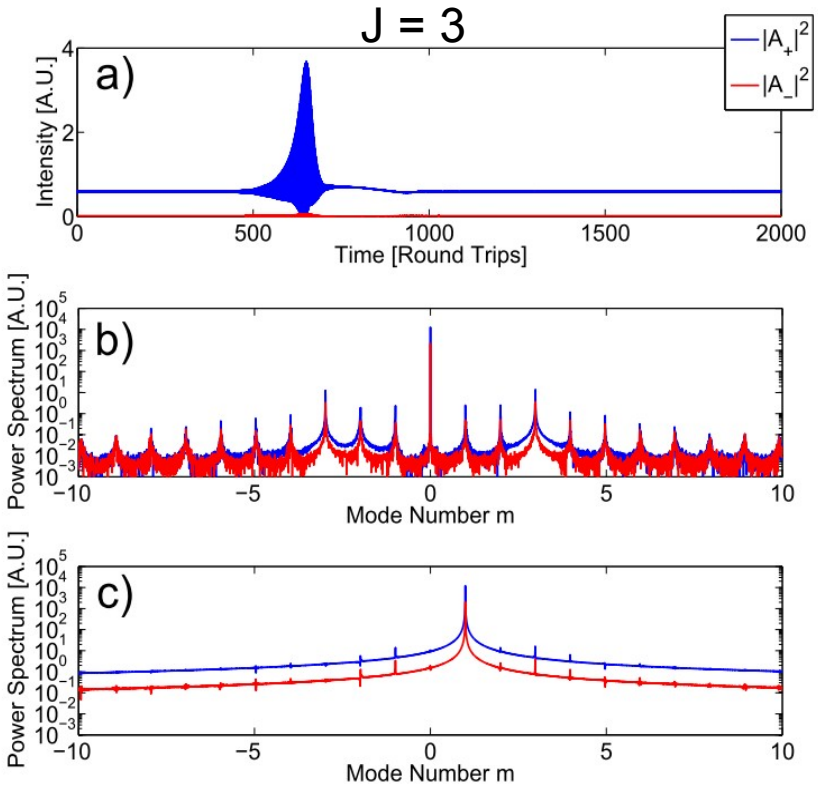

III. Longitudinal modal multistability in lasers

Fair comparison between Ring and FP lasers:

Both should work with the same degree of gain saturation, hence the pump density and the threshold pump density should be the same in both cases.

Ring: single pass on the cavity

FP: roundtrip

$$L_{Ring} = 2\, L_{FP}$$

$$g_{Ring} = 2\, g_{FP}$$
$$\gamma_{Ring} = 2\, \gamma_{FP}$$
$$\varepsilon_{Ring} = 2\, \varepsilon_{FP}$$
$$\eta_{Ring} = 2\, \eta_{FP}$$

III. Longitudinal modal multistability in lasers

Uniform Field Limit (UFL)

Ring laser

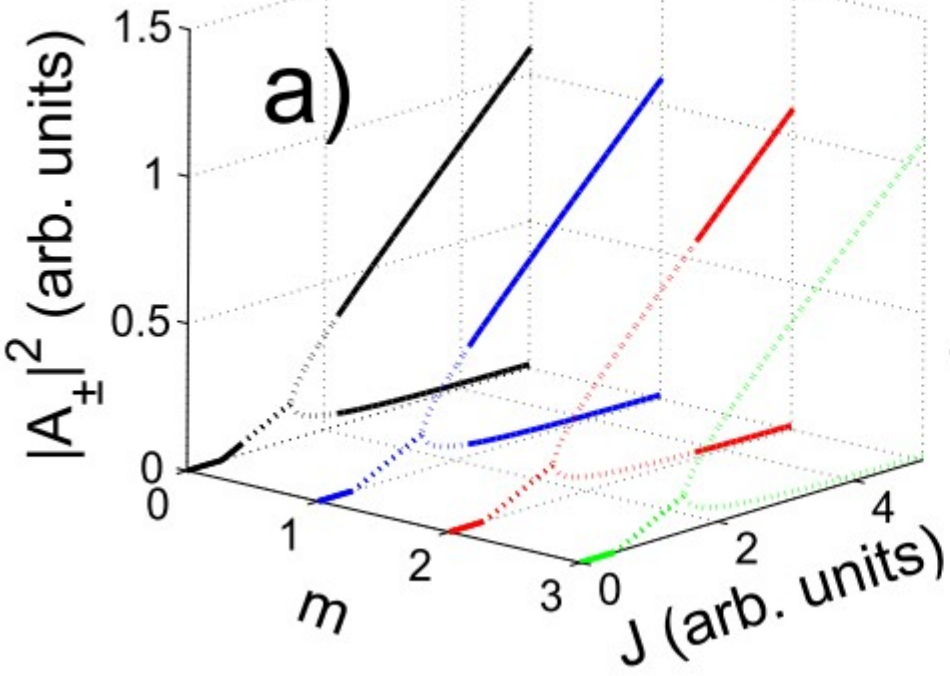

Fabry-Pérot laser

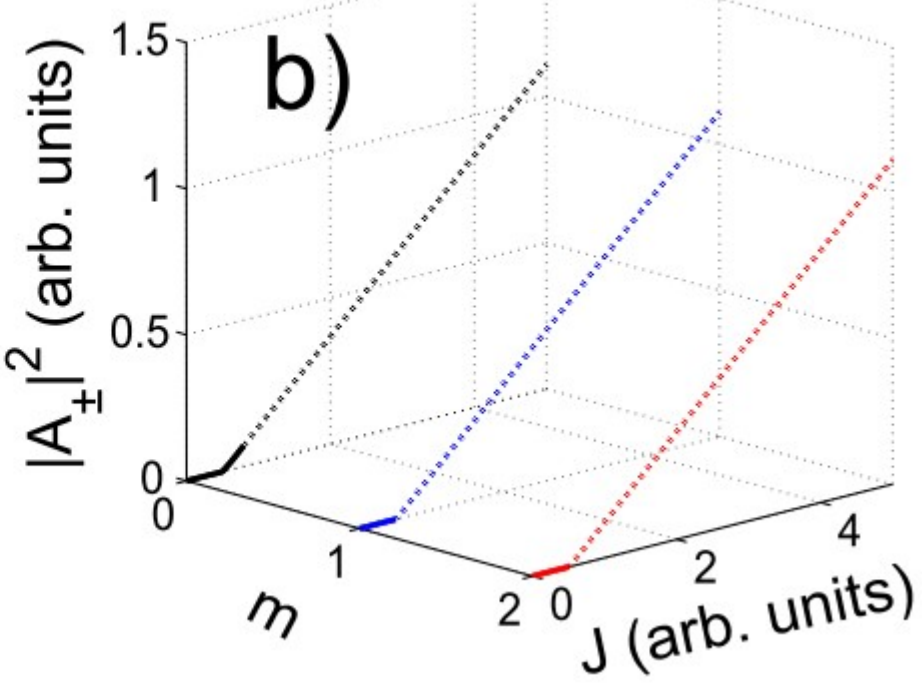

$t_{\pm} = 0$, $r_{\pm} = 0.99$, $\alpha = 1.01$

III. Longitudinal modal multistability in lasers

High losses lasers

Ring laser

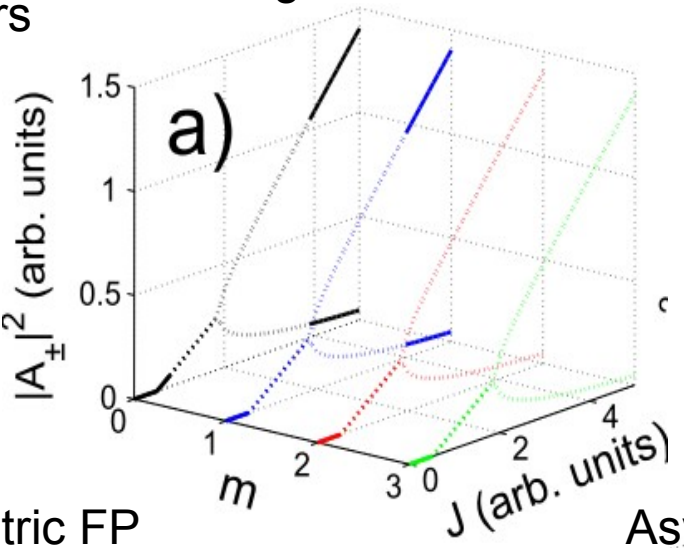

$g = 4$ $\quad \Delta = 0$

$t_\pm = 0.6$ $\quad \alpha = 1.55$

$r_\pm = 0.01$

$\varepsilon = 0.05$

$\eta = 10$

$\gamma = 250$

$\delta = 0$

Symmetric FP

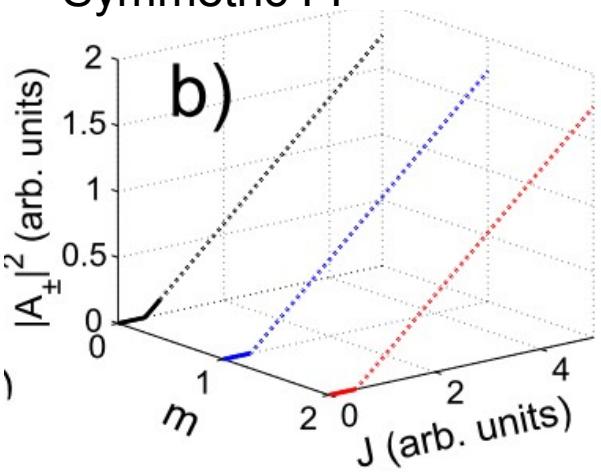

$t_\pm = 0$

$r_\pm = 0.6$

$\alpha = 0.51$

Asymmetric FP

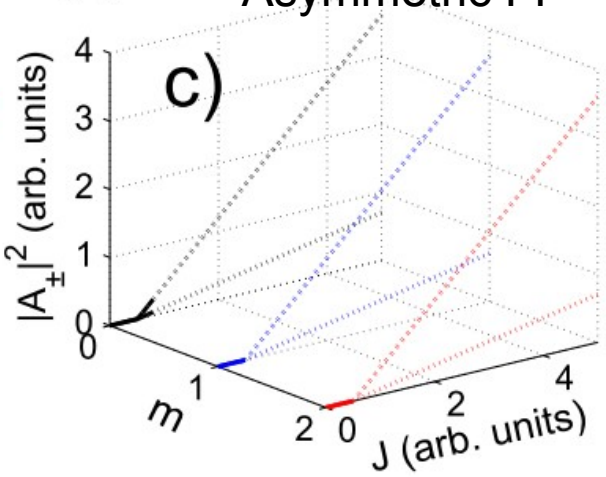

$t_\pm = 0$

$r_+ = 0.99$

$r_- = 0.2$

$\alpha = 0.21$

III. Longitudinal modal multistability in lasers

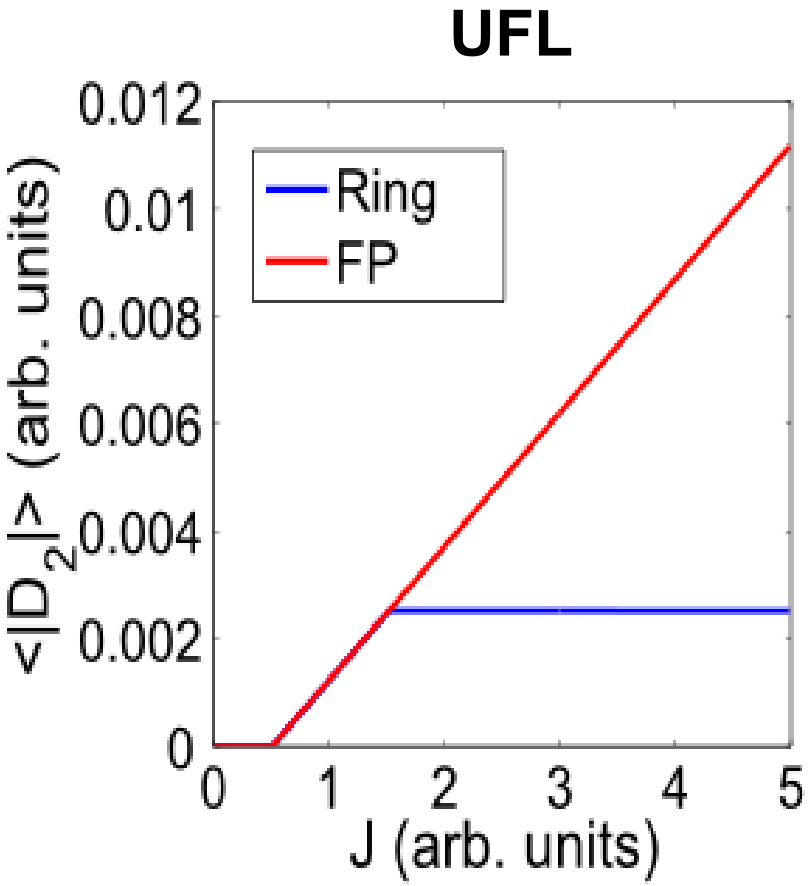

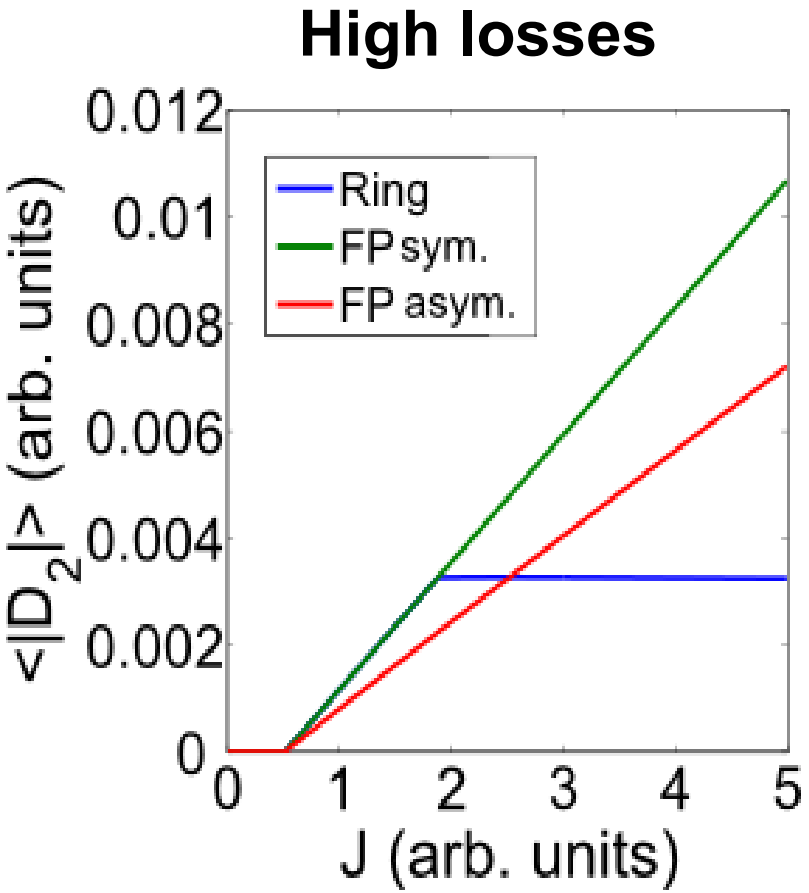

III. Longitudinal modal multistability in lasers

Symmetric FP

Asymmetric FP

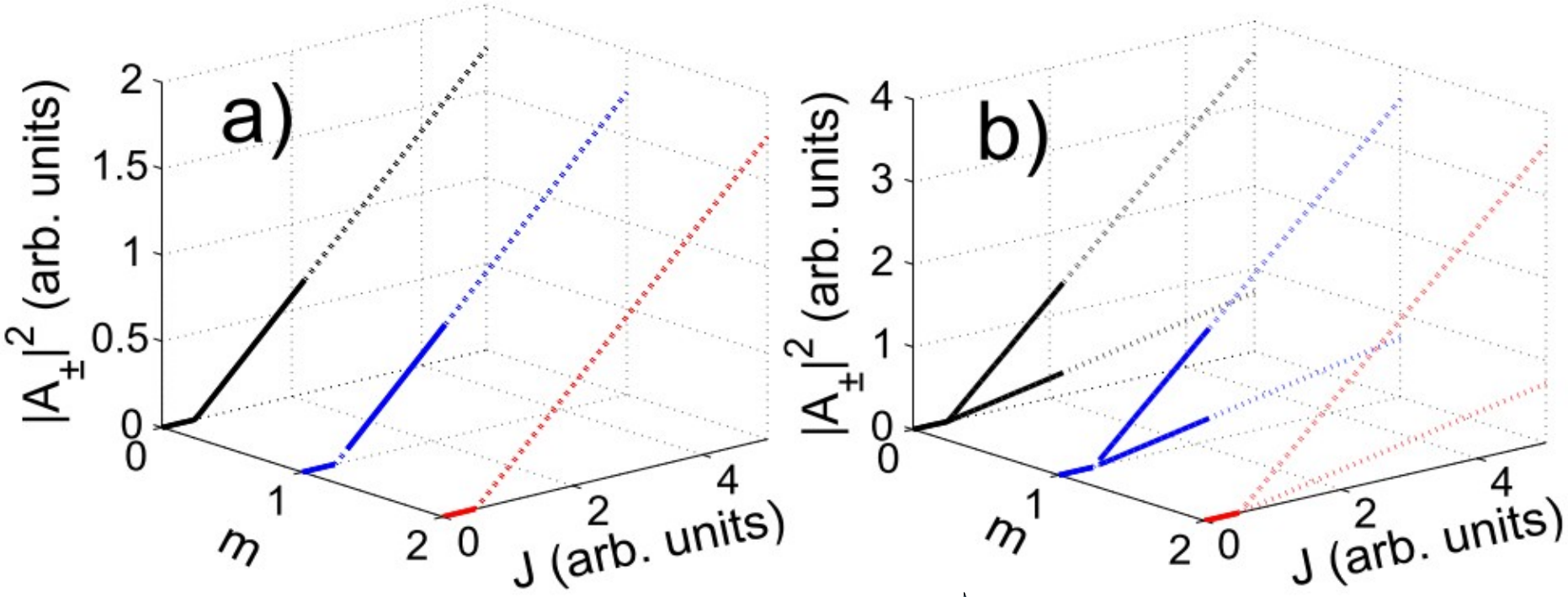

Increasing diffusion → $\eta = 10$ ⇒ Multistability in FPs

IFISC

IV. Conclusions

- We theoretically discuss the impact of the cavity configuration on the possible longitudinal mode multistability in homogeneously broadened lasers based on a general form of a Travelling Wave Model.

- The LSA perfomed can be exported to other dynamical systems involving PDEs.

- Multistability is more easily reached in Ring lasers than in FP lasers and is due to the different amounts of Spatial Hole Burning in each configuration.

  - In a high quality Ring with low reflectivities, the grating terms are small, then self-saturation is smaller than cross-saturation, and multistability appears.

  - In a FP configuration the grating effects are usually important, then self-saturation is bigger than cross-saturation and multistability is not allowed. This grating effect can be reduced by increasing difussion.

- Work in progress: Semiconductor material.

Thank you for your attention!

For details:

Pérez-Serrano et al. Phys. Rev. A **81**, 043817 (2010).

Pérez-Serrano et al. Opt. Express **19**, 3284 (2011).

Multimode Dynamics: C2.4 Talk 9:30h

Financial Support:

IOLOS

www.iolos.org

Govern de les Illes Balears

* Numerical methodology I

Monochromatic solutions solved numerically via a multidimensional shooting method:

A guess is proposed for the modal frequency ω_0 and the fields at s = 0, $A_{\pm}(0)$

Numerical integration in space (step = 1/N)
One obtains $A_{\pm}(1)$

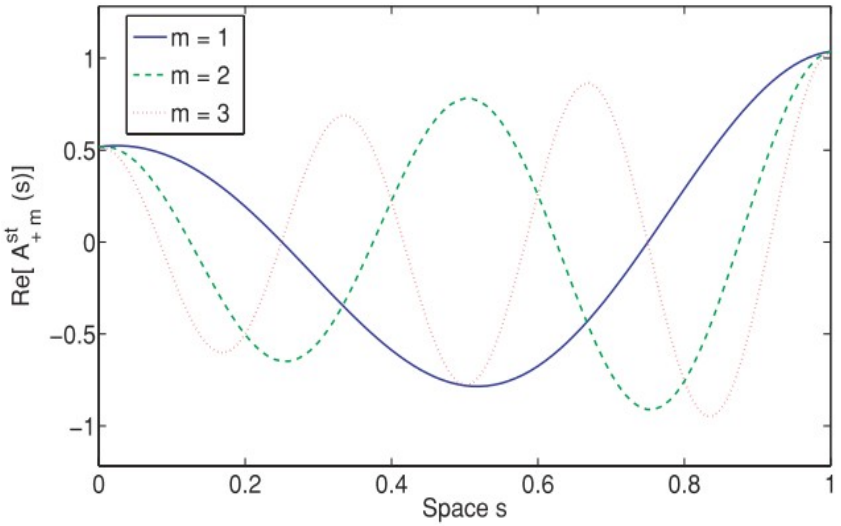

Verifying the boundary conditions a low dimensional Newton-Raphson computes a new guess for $A_{\pm}(0)$ and ω_0. The process is repeated until convergence.

Discretized modal profile

* Numerical methodology II (LSA)

Being **V*** a monochromatic solution, we go to the reference frame ω.

From the TWM (PDEs) we construct the evolution operator $\mathbf{U}(h,\mathbf{V}_n)$.

We use the temporal map $\mathbf{V}_{n+1} = \mathbf{U}(h,\mathbf{V}_n)$ to advance the state vector **V** a time step *h*, while verifying the Courant condition and cancelling numerical dissipation,
then $\mathbf{V}^*_{n+1} = \mathbf{U}(h,\mathbf{V}^*_n) = \mathbf{V}^*_n$

We consider all possible perturbations of $\mathbf{V} = \mathbf{V}^* + \delta\mathbf{V}$ finding the matrix $\mathbf{M} = \partial\mathbf{U}/\partial\mathbf{V}$
Where **M** is the linearized evolution operator.

We compute 11xN Floquet multipliers $\boldsymbol{z}_i$ of **M** $\quad \lambda_i = h^{-1} \ln \boldsymbol{z}_i$

* e.g. N = 256, standard PC using C++ routine based on *Octave*

Monochromatic solution → 1 s
Generating **M** → 10 s
Diagonalizing with QR decomposition → 60 s